



## Primary and secondary organic aerosols in 2016 summer of Beijing

Rongzhi Tang<sup>1</sup>, Zepeng Wu<sup>1</sup>, Xiao Li<sup>1</sup>, Yujue Wang<sup>1</sup>, Dongjie Shang<sup>1</sup>, Yao Xiao<sup>1</sup>,  
Mengren Li<sup>1</sup>, Limin Zeng<sup>1</sup>, Zhijun Wu<sup>1</sup>, Mattias Hallquist<sup>2</sup>, Min Hu<sup>1</sup>, Song Guo<sup>1,\*</sup>

<sup>1</sup>*State Key Joint Laboratory of Environmental Simulation and Pollution Control,  
College of Environmental Sciences and Engineering, Peking University, Beijing,  
100871, PR China*

<sup>2</sup>*Atmospheric Science, Department of Chemistry and Molecular Biology, University  
of Gothenburg, Sweden*

\* Correspondence to: Song Guo, [songguo@pku.edu.cn](mailto:songguo@pku.edu.cn)



## 1 Abstract

2 To improve the air quality, Beijing government has employed several air pollution  
3 control measures since 2008 Olympics. In order to investigate the organic aerosol  
4 sources after the implementation of these measures, ambient fine particulate matters  
5 were collected at a regional site Changping (CP) and an urban site Peking University  
6 Atmosphere Environment MonitoRing Station (PKUERS) during the “Photochemical  
7 Smog in China” field Campaign in summer of 2016. A chemical mass balance (CMB)  
8 modeling and the tracer yield method were used to apportion the primary and  
9 secondary organic sources. Our results showed that the particle concentration  
10 decreased significantly during the last a few years. The apportioned primary and  
11 secondary sources explained  $62.8 \pm 18.3\%$  and  $80.9 \pm 27.2\%$  of the measured OC at  
12 CP and PKUERS, respectively. Vehicular emissions served as the dominant sources.  
13 Except gasoline engine emission, the contributions of all the other primary sources  
14 decreased. Besides, the anthropogenic SOC, i.e. toluene SOC, also decreased,  
15 implying that deducting primary emission can reduce anthropogenic SOA. Different  
16 from the SOA from other regions in the world, where biogenic SOA was dominant,  
17 anthropogenic SOA was the major contributor to SOA, implying that deducting  
18 anthropogenic VOCs emissions is an efficient way to reduce SOA in Beijing. Back  
19 trajectory cluster analysis results showed that high mass concentrations of OC were  
20 observed when the air mass was from south. However, the contributions of different  
21 primary organic sources were similar, suggesting the regional particle pollution. The  
22 ozone concentration and temperature correlated well with the SOA concentration.  
23 Different correlations between day and night samples suggested the different SOA  
24 formation pathways. Significant enhancement of SOA with increasing particle water  
25 content and acidity were observed in our study, suggesting the aqueous phase  
26 acid-catalyzed reactions may be the important SOA formation mechanism in summer  
27 of Beijing.



## 28 **1. Introduction**

29 Beijing is the capital and a major metropolis of China. With the rapid economic  
30 growth and urbanization, Beijing is experiencing serious air pollution problems, and  
31 became one of the hotspots of PM<sub>2.5</sub> (particular matters with size smaller than 2.5µm)  
32 pollution in the world (Guo et al., 2014; Xiang et al., 2017; Tian et al., 2016). Due to  
33 the frequent haze events in Beijing, Beijing government has taken a series of control  
34 measures in recent years, especially after 2008 Olympics, which may greatly  
35 influence the primary and secondary particle sources. Therefore, elucidating the  
36 current contributions of primary particle sources as well as secondary particle sources  
37 is of vital importance. It is also important to compare with the previous results to  
38 evaluate the effectiveness of the control measures and shed light on the influence of  
39 the primary source emission control on the secondary aerosol formation.

40 Several studies regarding to the source apportionment of fine particles in Beijing have  
41 been conducted using multifarious methods during the last few years (Yu et al., 2013;  
42 Gao et al., 2014; Zheng et al., 2016b; Tan et al., 2014; Wang et al., 2009; Guo et al.,  
43 2013). Receptor model is a commonly used method to apportion the particle sources  
44 (Zhang et al., 2017; Zhou et al., 2017; Zhang et al., 2013; Song et al., 2006; Zheng et  
45 al., 2005). Elemental tracers were previously used to apportion particulate matter  
46 sources (Yu et al., 2013; Gao et al., 2014; Zheng et al., 2016b). However, elemental  
47 tracer-based method was unable to distinguish sources that mostly emit organic  
48 compounds instead of specific elements such as diesel/gasoline engines. Among all  
49 the apportionment methods, chemical mass balance (CMB) model was one of the  
50 most commonly used methods to apportion the primary organic sources of fine  
51 particulate matter (Zhang et al., 2017; Hu et al., 2015; Schauer et al., 1996). Organic  
52 tracers have been successfully used in several studies which aimed to quantify the  
53 main sources of Beijing (Liu et al., 2016; Guo et al., 2013; Wang et al., 2009). Wang  
54 et al. assessed the source contributions of carbonaceous aerosol during 2005 to 2007



55 (Wang et al., 2009). Guo et al. (Guo et al., 2013) and Liu et al. (Liu et al., 2016)  
56 apportioned the organic aerosol sources using CMB model in summer of 2008 and a  
57 severe haze event in winter of 2013. Both studies found that vehicle emission and coal  
58 combustion were the dominant primary sources of fine organic particles. Tracer-yield  
59 method has been considered as a useful tool to semi-quantify SOA derived from  
60 specific VOCs precursors (Guo et al., 2012; Zhu et al., 2017; Zhu et al., 2016; Tao et  
61 al., 2017; Hu et al., 2008). However, only a few studies have estimated secondary  
62 organic aerosol in Beijing. Yang et al. (Yang et al., 2016) estimated the biogenic SOC  
63 to OC during CAREBEIJING-2007 field campaign, and found that the SOC  
64 accounted for 3.1% of the measured OC. Guo et al. (Guo et al., 2012) illustrated the  
65 SOA contributions in 2008, and found that secondary organic carbon could contribute  
66 a great portion ( $32.5 \pm 15.9\%$ ) to measured organic carbon at the urban site. Ding et al.  
67 (Ding et al., 2014) used the tracer-yield method to investigate the SOA loading on a  
68 national scale and found that SOA, especially anthropogenic SOA played great role in  
69 major city clusters of China.

70 In this study, we quantified 144 kinds of particulate organic species, including  
71 primary and secondary organic tracers, at a regional site and an urban site of Beijing.  
72 A CMB modeling and the tracer yield method were used to apportion the primary and  
73 secondary sources of the organic aerosols in the 2016 summer of Beijing. The results  
74 were compared with the previous studies to evaluate the effectiveness of control  
75 measures on primary as well as secondary organic aerosols. Moreover, source  
76 apportionment results from different air mass origins according to the back trajectory  
77 clustering analysis were shown to investigate the influences of air mass from different  
78 directions on the fine organic particle sources. Influencing factors of SOA formation,  
79 i.e. temperature, oxidant concentration, aerosol water content, as well as particle  
80 acidity were also discussed in this study to improve our understanding of SOA  
81 formation under polluted environment.



## 82 2. Experimental

### 83 2.1 Sampling and Chemical Analysis

84 The measurements were conducted simultaneously at an urban site Peking University  
85 Atmosphere Environment MonitoRing Station (PKUERS, 39°59'21" N, 116°18'25" E)  
86 and a regional site Changping (CP, 40°8'24"N, 116°6'36" E) 40km north of PKUERS  
87 site during "Photochemical Smog in China" campaign, from May 16<sup>th</sup> to June 5<sup>th</sup>,  
88 2016 (see Fig. S1). The PKUERS site is set on the roof at an academic building on the  
89 campus of Peking University in the northwest of Beijing. CP site is located on the  
90 fourth floor of a building on the Peking University Changping campus of Changping.

91 Four-channel samplers (TH-16A, Tianhong, China) consisting of three quartz filter  
92 channel and one Teflon filter channel, were employed to collect 12-h aerosol samples  
93 at PKUERS and CP, respectively. The sampling flow rate was 16.7 L min<sup>-1</sup>. Teflon  
94 filters were weighed by a microbalance (Toledo AX105DR, USA) after a 24 h balance  
95 in an environmental controlled room (temperature 20 ± 1°C, relative humidity 40 ±  
96 3%) for gravimetric analysis. Teflon-based samples were extracted by deionized water  
97 to measure water-soluble inorganic compounds (WSICs), namely Na<sup>+</sup>, NH<sub>4</sub><sup>+</sup>, K<sup>+</sup>,  
98 Mg<sup>2+</sup>, Ca<sup>2+</sup>, NO<sub>3</sub><sup>-</sup>, SO<sub>4</sub><sup>2-</sup> and Cl<sup>-</sup> by DIONEX ICS-2500 and ICS-2000  
99 ion-chromatograph. One punch (1.45 cm<sup>2</sup>) of quartz-based sample was then cut off to  
100 analyze the EC and OC via thermal-optical method using Sunset Laboratory-based  
101 instrument (NIOSH protocol, TOT). The other two quartz filters were then extracted  
102 and analyzed for chemical composition and particulate organic matters. Some daytime  
103 and nighttime samples were combined to ensure the detection of most organic  
104 compounds. To better understand the chemical speciation, daytime samples were  
105 separated from nighttime samples.

106 Authentic standards were used to identify and quantify the organic compounds. The  
107 analytical methods used in this study referred to the previous work (Song et al., 2014).  
108 Briefly, the samples were first spiked with a mixture of internal standard, including



109 ketopinic acid (KPA), 20 kinds of deuterated compounds, and one carbon isotope  
110  $^{13}\text{C}$ -substituted compound. The filters were then ultrasonically extracted with  
111 methanol: dichloromethane (v:v=1:3) solvent in water bath (temperature < 30 °C) for  
112 3 times. Each time was 20 min. The extracts were filtered, and then concentrated  
113 using a rotary vacuum evaporator. An ultra-pure nitrogen flow was used to further  
114 concentrate the extracts into 0.5-1 ml. Each extracted solution was divided into two  
115 portions, one of which added BSTFA (BSTFA/TMCS = 99:1, Supelco) to convert  
116 polar organic compounds into trimethylsilylated derivatives. Afterwards, the  
117 derivatized and the untreated samples were analyzed by an Agilent 6890 GC-MS  
118 System (MSD GC-5973N) equipped with an Agilent DB-5MS GC column (30 m ×  
119 0.25 mm × 0.5 μm).

## 120 2.2 Source Apportionment

121 A chemical mass balance modelling developed by the U.S. Environmental Protection  
122 Agency (EPA CMB version 8.2) was applied to determine the apportion of the  
123 primary contribution of OC (Schauer et al., 1996). This receptor model solved a set of  
124 linear equations using ambient concentrations and chemical source profiles. CMB  
125 approach depends strongly on the representativeness of the source profile. In this  
126 study, five primary source profiles including vegetative detritus (Rogge et al., 1993),  
127 coal combustion (Zheng et al., 2005), gasoline engines (Lough et al., 2007), diesel  
128 engines (Lough et al., 2007) as well as biomass burning (Sheesley et al., 2007) were  
129 input into the model. Fitting species including EC, n-alkanes, levoglucosan,  
130  $17\beta(\text{H})\text{-}21\alpha(\text{H})\text{-norhopane}$ ,  $17\alpha(\text{H})\text{-}21\beta(\text{H})\text{-hopane}$ , benzo(b)fluoranthene,  
131 benzo(k)fluoranthene, benzo(e)pyrene, benzo(ghi)perylene, indeno(1,2,3-cd)pyrene.  
132 The criteria for acceptable fitting results included the square regression coefficient of  
133 the regression equation  $R^2 > 0.85$  as well as the sum of square residual Chi-square  
134 value  $\chi^2 < 4$ .



135 The tracer yield method was used to estimate the contributions of biogenic and  
136 anthropogenic secondary organic aerosols using fixed tracers to SOC ratio ( $f_{\text{SOC}}$ )  
137 based on laboratory experiments, which was  $0.155 \pm 0.039$  for isoprene,  $0.231 \pm 0.111$   
138 for  $\alpha$ -pinene,  $0.0230 \pm 0.0046$  for  $\beta$ -caryophyllene and  $0.0079 \pm 0.0026$  for toluene  
139 (Kleindienst et al., 2007). The uncertainties of the estimation mainly derived from the  
140 impurity in choosing the organic tracer compounds as well as the idealization of the  
141 single-valued tracer mass fractions, which have been comprehensively discussed by  
142 previous studies (Yttri et al., 2011; El Haddad et al., 2011) (Song et al., 2014). Despite  
143 of its large uncertainties, the tracer-yield method was considered as a useful approach  
144 up to now to roughly estimate the SOA contributions derived from individual  
145 hydrocarbon precursors.

### 146 **3. Gaseous pollutants and particle chemical composition**

#### 147 **3.1 Gaseous pollutants and meteorological conditions of the observation period**

148 Mixing ratios of gaseous pollutants and meteorological conditions during the  
149 observation period were shown in Fig. S2 and Table S1. Compared with the results in  
150 summer of 2010 (Zheng et al., 2016a), the gaseous mixing ratios  $\text{SO}_2$  and CO were  
151 lower than before owing to the desulfurization efforts made by the government.  
152 Higher concentrations of NO and  $\text{NO}_2$  were caused by the increasing number of  
153 vehicles. The increment of ozone indicated the importance of secondary pollution.  
154 Clearly, ozone concentration at CP was higher than that of PKUERS while other  
155 pollutants were lower.

156 During the campaign, the average wind speed was low, showing average values of  $2.3$   
157  $\pm 1.4$  m/s and  $2.4 \pm 1.5$  m/s at CP and PKUERS, respectively. The diurnal variations  
158 of wind directions and speeds are exhibited in Fig. S2. The prevailing wind was from  
159 south, with higher wind speed during the daytime.

160 To explore the influence of the air masses from different directions on fine particle  
161 loading and sources, back trajectory analysis was performed using National Oceanic



162 and Atmospheric Administration (NOAA) Hybrid Single Particle Lagrangian  
163 Integrated Trajectory (HYSPLIT) model. We calculated 36 h air mass back  
164 trajectories arriving at two sampling site during the observation period using the  
165 HYSPLIT-4 model with a  $1^\circ \times 1^\circ$  latitude-longitude grid and the final meteorological  
166 database. The model was run with the starting time of 0:00, 4:00, 8:00, 12:00, 16:00,  
167 and 20:00 UTC). The arrival level was set at 200 m above ground level. The method  
168 used in trajectory clustering was based on GIS-based software TrajStat  
169 (<http://www.meteothinker.com/TrajStatProduct.aspx>). 36-h back trajectories starting at  
170 200 m above ground level in CP and PKUERS were calculated every 4 hours during  
171 the entire campaign and then clustered according to their similarity in spatial  
172 distribution using the HYSPLIT4 software. Three-cluster solution was adopted as  
173 shown in Fig. S3. The three clusters were defined as Far North West (Cluster 1, Far  
174 NW), Near West North (Cluster2, Near WN), and South (Cluster 3). South cluster was  
175 found to be the most frequent one, accounting for 52% at CP and 64% at PKUERS.  
176 Clusters Far NW and Near NW accounted for 17% and 31%, 17% and 19% at CP and  
177 PKUERS, respectively.

### 178 **3.2 Overview of PM<sub>2.5</sub> chemical composition**

179 In this study, daily PM<sub>2.5</sub> concentrations fluctuated dramatically from  $6.7 \mu\text{g m}^{-3}$  to  
180  $80.3 \mu\text{g m}^{-3}$  at CP, and from 9.6 to  $82.5 \mu\text{g m}^{-3}$  at PKUERS, respectively. A paired  
181 t-test was used to compare the mass concentrations at two sites. The results indicate  
182 that the mass concentrations showed statistically non-significant difference,  
183 suggesting the regional particle pollution in Beijing. PM<sub>2.5</sub> mass concentrations during  
184 the summer of 2008 to 2016 in Beijing are summarized in Table 1. Guo et al. (Guo et  
185 al., 2013) reported the average PM<sub>2.5</sub> concentrations during the summers of 2000 to  
186 2008, which showed distinct decreasing tendency during 2000-2006 and then slightly  
187 increased in 2007 due to unfavorable meteorological conditions. To better understand  
188 the variation tendency of the PM<sub>2.5</sub> in the summer of Beijing, we compared the fine  
189 particle matter data since 2008. Compared with 2008, the PM<sub>2.5</sub> concentrations



190 decreased from  $92.3 \pm 44.7 \mu\text{g m}^{-3}$  to  $88.2 \mu\text{g m}^{-3}$  in 2009 and  $62.7 \mu\text{g m}^{-3}$  in 2010.  
191 The mass concentration continued falling to  $45.5 \mu\text{g m}^{-3}$  in 2016. This decreasing is  
192 attributed to the drastic emission control measures implemented by the Beijing  
193 government since 2012. In spite of the prominent decrease of the  $\text{PM}_{2.5}$  mass  
194 concentrations, the aerosol loading in Beijing was still much higher than that in  
195 developed countries (Tai et al., 2010; Barmpadimos et al., 2012; Park and Cho, 2011).

196 Fig. S4 showed the chemical composition of  $\text{PM}_{2.5}$ . In general, organic particulate  
197 matters (OM,  $\text{OC} \times 1.6$ ) and sulfate were the two dominant components, accounting for  
198 more than 50% of the  $\text{PM}_{2.5}$  mass concentration during the field campaign. The  
199 average concentration of total WSICs for CP was  $17.4 \pm 11.5 \mu\text{g m}^{-3}$ , higher than that  
200 of PKUERS ( $12.2 \pm 8.5 \mu\text{g m}^{-3}$ ). Among the WSICs, secondary inorganic ions (sulfate,  
201 nitrate, and ammonium) were the most abundant compounds, indicating secondary  
202 particles played great roles in the summer of Beijing. The higher sulfate proportion  
203 could be explained by the increased photochemical conversion of sulfur dioxide to  
204 sulfate aerosol (Xiang et al., 2017).

205 Carbonaceous aerosols, i.e. organic carbon (OC) and elemental carbon (EC) were also  
206 great contributors to  $\text{PM}_{2.5}$  concentrations. Higher proportion of OC and EC at  
207 PKUERS demonstrated severe carbonaceous pollution in urban Beijing, which might  
208 have close correlation with the higher traffic flow, coal/wood combustion by residents  
209 and industrial emissions (Wang et al., 2006; Dan et al., 2004; Cao et al., 2004).  
210 Comparison of the OC, EC concentrations from 2008 to 2016 were also listed in Table  
211 1. Unlike  $\text{PM}_{2.5}$ , OC concentration at PKUERS showed a higher OC concentration  
212 ( $11.0 \pm 3.7 \mu\text{g m}^{-3}$ ) compared with that in 2008 ( $9.2 \pm 3.3 \mu\text{g m}^{-3}$ ), suggesting organic  
213 aerosol pollution becomes more and more important. EC concentration decreased  
214 dramatically to  $0.7 \pm 0.5 \mu\text{g m}^{-3}$  at CP and  $1.8 \pm 1.0 \mu\text{g m}^{-3}$  at PKUERS, which  
215 showed the lowest value since 2000. This could be attributed to the implementation of  
216 air pollution prevention and control action plan enacted by the state council since  
217 2013.



218 To evaluate the influences of the air masses from different directions on the  $PM_{2.5}$   
219 loadings during the campaign, three categories were divided according to the back  
220 trajectory clustering analysis (See Fig. S5). In general, cluster south represented the  
221 most polluted air mass origin followed by clusters Near WN and Far NW, which was  
222 in accordance with previous studies demonstrating severe aerosol pollution in  
223 southerly air flow in summer of Beijing (Huang et al., 2010; Sun et al., 2010).

### 224 **3.3 Concentration of particulate organic species from different air mass origins**

225 The organic species (except secondary organic tracers) were divided into 12  
226 categories. Their concentrations in different directions according to the back trajectory  
227 clustering were shown in Fig. S6. Detailed information for each class at the two sites  
228 could be found in the supplementary material (Fig. S7). Cluster south showed higher  
229 particulate organic matter concentration, followed by cluster near WN and far NW,  
230 indicating more severe aerosol pollution from the south. Our result consists with the  
231 previous studies that more pollution emissions are from the south area of Beijing than  
232 those from the north (Wu et al., 2011; Zhang et al., 2009).

233 Dicarboxylic acid was the most abundant species among all the components,  
234 demonstrating the great contribution of the secondary formation to the organic  
235 aerosols in the summer of Beijing (Guo et al., 2010). A series of n-alkanes ranging  
236 from C12 to C36 were analyzed. Their distribution during the observation period was  
237 shown in Fig. S7 (a). The maximum-alkane concentration species ( $C_{max}$ ) were C27  
238 and C29. The odd carbon preference was an indicative of biogenic sources (vegetative  
239 matters and biomass burning) (Huang et al., 2006; Rogge et al., 1993). In this study,  
240 total PAHs were much lower than previous studies in summer of Beijing, suggesting  
241 the effectiveness of the control strategies since 2013 (Wang et al., 2009). According to  
242 Fig. S7 (c), five ring PAHs were dominant species among all the species, followed by  
243 four-ring and six-ring PAHs. In total, four to six ring PAHs had higher abundancy,  
244 accounting for more than 60% of the total PAHs. The result was much similar with



245 previous studies that the distribution of PAHs was impacted by the volatility of PAHs  
246 and the temperature (Wang et al., 2009; Guo et al., 2013). Saccharide was considered  
247 to originate from biomass burning (Simoneit et al., 1999). In this study, we quantified  
248 three sugar compounds including levoglucosan, manosan and galactosan, in which  
249 levoglucosan was considered as a good tracer for biomass burning. The average daily  
250 mass concentration of levoglucosan at CP and PKUERS were  $53.03 \pm 39.26 \text{ ng m}^{-3}$   
251 and  $59.87 \pm 38.93 \text{ ng m}^{-3}$ , respectively. It's worth mentioning that the levoglucosan  
252 concentration was the lowest in recent years (Cheng et al., 2013; Guo et al., 2013).  
253 Hopanes have been considered as markers for oil combustion (Lambe et al., 2009),  
254 vehicles (i.e. gasoline-powered and diesel-powered engine) (Cass, 1998; Lough et al.,  
255 2007) and coal combustion (Oros and Simoneit, 2000). Nevertheless, contributions of  
256 coal combustion to hopanes were much less than that of vehicle exhaustion.  
257 Concentrations of quantified hopanes including  $17\alpha(\text{H})$ -22,29,30-trishopane,  
258  $17\beta(\text{H})$ -21 $\alpha(\text{H})$ -norhopane, and  $17\alpha(\text{H})$ -21 $\beta(\text{H})$ -hopane of CP and PKUERS are  
259 shown in Fig. S7(d). The total average concentrations of hopanes were  $3.05 \pm 1.53 \text{ ng}$   
260  $\text{m}^{-3}$  for CP and  $3.90 \pm 2.06 \text{ ng m}^{-3}$  for PKUERS. The hopanes concentrations at urban  
261 site PKUERS were much higher than that of CP, which could probably explained by  
262 the heavier vehicle emissions in the urban area. The concentrations of primary organic  
263 tracers used in CMB model were listed in Table S2.

### 264 **3.4 Biogenic and anthropogenic SOA tracers**

265 Table S3 compared the SOA tracers measured in this work with those in other regions  
266 in the world as well as that observed in Beijing 2008. The sites for comparison  
267 include an urban background site at Indian Institute of Technology Bombay, Mumbai,  
268 India (IITB) (Fu et al., 2016), an outflow region of Asian aerosols and precursors  
269 Cape Hedo, Okinawa, Japan (CH) (Zhu et al., 2016), a residential site at Yuen Long,  
270 Hong Kong (YL) (Hu et al., 2008), three industrial sites at Cleveland Ohio (CL, data  
271 was averaged among the three sites), a suburban site in the Research Triangle Park



272 North California (RTP). The detailed information about these sites were summarized  
273 in the supplementary material.

274 Three isoprene-SOA tracers i.e. two 2-methyltetrols (2-methylthreitol and  
275 2-methylerythritol) and 2-methylglyceric acid were detected. The summed  
276 concentration of the isoprene-SOA tracers ranged from 3.7 to 62.3 ng m<sup>-3</sup> at CP and  
277 8.6 to 46.5 ng m<sup>-3</sup> at PKUERS. The concentration was higher than that of IITB and  
278 CH. Compared with the isoprene-SOA tracers in 2008, the concentrations in 2016  
279 were lower.

280 Nine  $\alpha$ -pinene tracers were identified. The sum of the tracers ranged from 20.9 to  
281 282.3 ng m<sup>-3</sup> at CP and 50.0 to 161.4 ng m<sup>-3</sup> at PKUERS, which had similar  
282 distribution pattern with that measured in 2008 Beijing and YL. The total  $\alpha$ -pinene  
283 tracer concentrations were lower than those in 2008, while still much higher than the  
284 concentrations in other regions of the world.

285  $\beta$ -caryophyllinic acid is one of the oxidation products of  $\beta$ -caryophyllene which is  
286 considered as a tracer for  $\beta$ -caryophyllene SOA. In this study,  $\beta$ -caryophyllinic acid  
287 concentrations ranged from 1.4 to 16.7 ng m<sup>-3</sup> at CP, and 0.9 to 12.0 ng m<sup>-3</sup> at  
288 PKUERS, with average daily average concentrations of  $6.1 \pm 3.5$  ng m<sup>-3</sup> and  $6.0 \pm 2.8$   
289 ng m<sup>-3</sup> for CP and PKUERS, respectively. The values were lower than those at YL and  
290 RPT, higher than that measured at Yufa and PKUERS in 2008.

291 2,3-Dihydroxy-4-oxopentanoic acid is deemed as a tracer for toluene SOA. Our  
292 results showed that the 2,3-Dihydroxy-4-oxopentanoic acid concentration was  $9.7 \pm$   
293  $7.3$  ng m<sup>-3</sup> at CP and  $11.0 \pm 3.7$  ng m<sup>-3</sup> at PKUERS. Compared with other regions of  
294 the world, the concentrations of 2,3-Dihydroxy-4-oxopentanoic acid was much higher,  
295 implying higher contributions of anthropogenic sources at Beijing. However, the  
296 concentrations in CP were lower than that of PKUERS.



## 297 **4. Primary sources and secondary formation of organic aerosols**

### 298 **4.1 Contributions of primary and secondary organic aerosols**

299 A CMB model and the tracer-yield method were used to quantify the contributions of  
300 primary and secondary sources to the ambient organic carbon (See Fig. 1). On  
301 average, the primary sources accounted for  $42.6 \pm 15.4\%$  and  $50.4 \pm 19.1\%$  of the  
302 measured OC at CP and PKUERS, respectively. The vehicle emissions were the  
303 dominant primary sources, with the contributions of  $28.8 \pm 14.8\%$  and  $37.6 \pm 19.3\%$   
304 at PKUERS and CP, respectively, implying the urgency to control vehicular  
305 exhaustion in urban areas. Despite of the lower contribution of the gasoline exhaust at  
306 PKUERS, the mass concentration of the gasoline exhaust was higher compared with  
307 that of CP given the higher OC loading at PKUERS. The contributions of biomass  
308 burning were  $3.9 \pm 2.6\%$  and  $5.0 \pm 2.2\%$  at CP and PKUERS, respectively, showing  
309 the higher concentrations at night. The drastic change of the biomass burning  
310 contribution in CP at night was due to occasional burning activities at night. Coal  
311 combustion contributed  $5.8 \pm 5.5\%$  and  $4.6 \pm 2.6\%$  of the measured OC at CP and  
312 PKUERS. The higher contribution at CP was due to more burning activities in the  
313 suburban areas.

314 The secondary organic sources accounted for  $20.2 \pm 6.7\%$  of the organic carbon at CP,  
315 with  $1.6 \pm 0.4\%$  from isoprene,  $4.4 \pm 1.5\%$  from  $\alpha$ -pinene,  $2.7 \pm 1.0\%$  from  
316  $\beta$ -caryophyllene and  $12.5 \pm 3.4\%$  from toluene. As for PKUERS, the secondary  
317 organic sources took up  $30.5 \pm 12.0\%$  of the measured OC, in which isoprene was  
318 responsible for  $2.3 \pm 0.9\%$ ,  $\alpha$ -pinene for  $5.6 \pm 1.9\%$ ,  $\beta$ -caryophyllene for  $3.6 \pm 2.6\%$   
319 and toluene for  $19.0 \pm 8.2\%$ . Haque et al. (Haque et al., 2016) used tracer-based  
320 method to apportion the organic carbon and results showed that the biogenic SOC was  
321 responsible for 21.3% of the total OC with isoprene SOC contributing 17.4%,  
322  $\alpha/\beta$ -pinene SOC contributing 2.5% and  $\beta$ -caryophyllene SOC contributing 1.4% in the  
323 summer of Alaska, implying the significant contributions of the biogenic SOA to the



324 loading of the organic aerosol. Our results exhibited that the biogenic SOA  
325 concentration was comparable or even high than that at some forest sites in other  
326 places of the world (Miyazaki et al., 2012; Stone et al., 2012; Claeys et al., 2004;  
327 Kourtchev et al., 2008). The SOA formation mechanism is complicated. A possible  
328 reason is the high oxidation capacity in China. More work is still needed to  
329 investigate the SOA formation mechanism under Air Pollution Complex in China.

330 Stone et al. (Stone et al., 2009) discovered that primary and secondary sources  
331 accounted for  $83 \pm 8\%$  of the measured organic carbon, with primary sources  
332 accounted for  $37 \pm 2\%$  and SOC contributed for  $46 \pm 6\%$  with  $16 \pm 2\%$  from biogenic  
333 gas-phase precursors and  $30 \pm 4\%$  from toluene using CMB model and tracer-based  
334 method at Cleveland with heavy industries, implying that anthropogenic sources  
335 played great roles in the formation of SOA. Our results showed a similar with the  
336 results published by Stone et al., where anthropogenic sources i.e. toluene derived  
337 SOC dominated the apportioned SOC. Our research revealed an important point that  
338 controlling SOA seems feasible in the developing countries like China. It is difficult  
339 to control SOA in developed countries, since biogenic SOA are dominant. However,  
340 deducting anthropogenic precursors may be an efficient way to reduce the SOA  
341 pollution where anthropogenic SOA is dominant. On average,  $62.8 \pm 18.3\%$  and  $80.9$   
342  $\pm 27.2\%$  of the measured OC were apportioned at CP and PKUERS, respectively.  
343 About  $36.3 \pm 18.1\%$  and  $29.3 \pm 15.6\%$  of the OC sources remained unknown, which  
344 were probably composed of uncharacterized primary or secondary sources. Further  
345 research is needed to explain the unapportioned sources of OC.

346 Due to the drastic emission control measures taken by the Beijing government, the  
347 primary and secondary sources in Beijing may change greatly. Fig. 2 displayed the  
348 comparison of the sources between 2008 and 2016 at the same site PKUERS. We  
349 compared the average contributions by percentage rather than the mass concentration.  
350 In general, primary sources contributed  $50.4 \pm 19.1\%$  of the measured OC in 2016,  
351 closely correlated to the increasing contribution of vehicular emissions. Gasoline



352 engines accounted for 18% of the measured OC, showing an enhancement of 80%  
353 with respect to 2008. This might be related to the rising number of the vehicles in  
354 Beijing. In comparison, diesel exhaust decreased by 12.5% due to the strict control  
355 measures made by the government. A 28.5% and 20% reduction of coal combustion  
356 and biomass burning could also be found due to the drastic measures made by the  
357 government. Compared with 2008, contributions of secondary organic aerosol  
358 decreased by 29.4%. However, the contribution of toluene SOC was the highest  
359 among the apportioned SOC, which was different from the results of the most  
360 developed countries in the world. In summary, the contributions of most POA  
361 decreased in recent years, except for gasoline exhaust, indicating more efforts should  
362 be made to control the gasoline emission. The apportioned SOC was also decreased  
363 with toluene SOC served as the dominant source. Our results revealed that deducting  
364 anthropogenic precursors may be an efficient way to control SOA pollution in China.

#### 365 **4.2 Organic aerosol sources from different air mass origins**

366 The regional sources and transport of air pollutants exert profound impacts on air  
367 quality of Beijing. To better understand the regional impacts on the primary and  
368 secondary aerosol sources of Beijing, source apportionment results when air mass  
369 from different origins were shown in Fig. 3. Vehicular emissions i.e. gasoline and  
370 diesel exhaust showed identical contributions from different air mass origins (31.0%  
371 from south vs 31.3% from Near WN vs 31.7% from Far NW) at PKUERS,  
372 demonstrating the vehicular pollution could mostly be attributed to the vehicular  
373 emission at the local site. However, the contribution of vehicular emission at CP  
374 showed significant difference from different air mass origins, with lowest contribution  
375 when air mass was from far northwest. This might be explained by regional transport  
376 from different directions. Comparable contributions of coal combustion and biomass  
377 burning were found at CP and PKUERS from different air mass origins, implying the  
378 regional pollution in Beijing. Similarly, biogenic SOC showed similar contributions  
379 from different air mass origins both at the regional site and the urban site. From all the



380 directions, the toluene SOC (anthropogenic source) was the largest contributor to  
381 apportioned SOC, with higher concentrations at the urban site PKUERS. On the  
382 whole, most of the sources showed comparable contribution from different air mass  
383 origins, implying the pollution in Beijing was regional.

#### 384 **4.3 Influencing factors for secondary organic aerosol formation in the summer of** 385 **Beijing**

386 Laboratory experiments have revealed that several factors can influence the SOA  
387 formation, e.g. oxidants (OH radical, ozone etc.), temperature, humidity, particle  
388 water content and acidity. In this work, the relationships between estimated SOA and  
389 these factors were investigated to better understand the SOA formation in Beijing.

#### 390 **SOA formation from ozonolysis**

391 Ozone is considered as an important oxidant for SOA formation. Fig. 4 (a)(b) showed  
392 the correlation with ozone mixing ratio and SOC. It is clear that SOC increased  
393 significantly with the increasing of ozone mixing ratio, which is consistent with  
394 previous studies in Beijing (Guo et al. 2012). Different correlations were found  
395 between day and night samples, with better correlation for the daytime samples at  
396 both sites, implying SOA may have other formation mechanism at night other than  
397 ozonolysis. At CP, the growth rate of SOC with O<sub>3</sub> was similar for day and night  
398 samples, which was 0.02 μg m<sup>-3</sup> per ppbv ozone. For PKUERS, the increment rate of  
399 the SOC towards ozone was 0.04 μg m<sup>-3</sup> and 0.02 μg m<sup>-3</sup> per ppbv ozone at day and  
400 night, respectively.

#### 401 **Influence of temperature and relative humidity on SOA formation**

402 Temperature was considered as a great influencing factor on SOA formation. On the  
403 one hand, higher temperature promoted the evaporation of the semi volatile SOA. On  
404 the other hand, high-temperature conditions would favor the oxidation, which would  
405 accelerate the SOA formation (Saathoff et al., 2009). Fig. 4 (c) (d) showed the



406 variation of SOC concentrations with the temperature. In this study, SOC  
407 concentration showed positive correlation with temperature at CP and PKUERS,  
408 demonstrating that temperature favors the SOA formation in the summer of Beijing.  
409 Moreover, different correlation of the day and the night samples imply the different  
410 pathways of SOA formation. However, poor relations could be found between SOC  
411 and RH.

#### 412 **Effects of aqueous-phase acid catalyzed reactions on SOA formation**

413 Aerosol water and acidity have been considered to have great impact on the  
414 aqueous-phase SOA formation (Cheng et al., 2016). To figure out the influences of  
415 water content and aerosol acidity on the aqueous-phase reactions, ISORROPIA-II  
416 thermodynamic equilibrium model was used (Surratt et al., 2007). The model was set  
417 at forward mode, based on the concentrations of particle phase  $\text{Na}^+$ ,  $\text{NH}_4^+$ ,  $\text{K}^+$ ,  $\text{Mg}^{2+}$ ,  
418  $\text{Ca}^{2+}$ ,  $\text{NO}_3^-$ ,  $\text{SO}_4^{2-}$ ,  $\text{Cl}^-$  and gaseous  $\text{NH}_3$  as well as ambient temperature and RH.

419 Results showed that the average aerosol water content at CP was  $3.87 \pm 3.73 \mu\text{g m}^{-3}$ ,  
420 higher than that at PKUERS ( $1.83 \pm 1.81 \mu\text{g m}^{-3}$ ). The water content was lower in  
421 2016 than that in 2008. The estimated SOC concentration showed good correlations  
422 with water content at both sites. Compared with CP, the correlation factor in PKUERS  
423 was better, implying that aqueous phase reaction may be more important in the urban  
424 area. Different correlation could be found at different liquid water contents, especially  
425 for CP, where liquid water content spanned a wide range, implying that different  
426 mechanisms may exist at different liquid water content.

427 In this study, modeled  $\text{H}^+$  concentration and SOC showed significant correlation  
428 ( $p < 0.05$ ) at the two places, which indicated that acid-catalyzed reaction might provide  
429 a crucial pathway for the SOA formation in the summer of Beijing. Laboratory studies  
430 showed that acid-catalyzed reactive uptake might play great role in the enhancement  
431 of SOA (Zhang et al., 2014; Surratt et al., 2010; Jang et al., 2002). However, contrary  
432 conclusions were made by other group, demonstrating the inconsistency of the aerosol



433 acidity and the SOA formation (Wong et al., 2015; Kristensen et al., 2014). The  
434 contradiction might give the facts that the impacts of the acidity on the SOA loading  
435 varied from place to place, determined by the specific environmental conditions.  
436 Linear regression showed that the enhancement of SOC with modeled  $H^+$   
437 concentration were at a value of  $0.02 \mu\text{g m}^{-3}$  per  $\text{nmol H}^+$ , which was lower than the  
438 previous results ( $0.046$  for PKUERS, and  $0.041$  for Yufa, 2008). Offenberg et al.  
439 (Offenberg et al., 2009) discovered good correlation between SOC and  $[H^+]_{\text{air}}$ , with  
440  $R^2$  value of  $0.815$ . Besides, a one  $\text{nmol m}^{-3} [H^+]_{\text{air}}$  would give rise to  $0.015 \mu\text{g m}^{-3}$   
441 SOC increase from the oxidation of  $\alpha$ -pinene in the chamber experiment. In the  
442 present work, different correlations could be found at different modeled  $H^+$   
443 concentrations where apportioned SOC increased significantly as the  $H^+$   
444 concentration increased and then increased slowly at a certain level, showing gradient  
445 growth at different hydrogen-ion concentrations. Therefore, aqueous phase  
446 acid-catalyzed reactions may influence the SOA formation through different  
447 mechanisms at varied level of liquid water concentration and aerosol acidity.

## 448 5. Conclusion

449 High concentrations of fine particles were observed during the “Campaign on  
450 Photochemical Smog in China”, with the average mass concentrations of  $45.48 \pm$   
451  $19.78 \mu\text{g m}^{-3}$  and  $42.99 \pm 17.50 \mu\text{g m}^{-3}$ , at CP site and PKUERS site, respectively.  
452 Compared with previous studies, the concentrations of  $\text{PM}_{2.5}$ , EC and estimated SOC  
453 decreased significantly, due to the drastic measures implemented by the government  
454 in the recent years. However, OC showed a higher concentration, suggesting  
455 particulate organic matters become more and more important in Beijing. CMB  
456 modeling and tracer-yield method were used to apportion the primary and secondary  
457 organic aerosol sources. The apportioned primary and secondary OC accounted for  
458  $62.8 \pm 18.3\%$  and  $80.9 \pm 27.2\%$  of the measured OC at CP and PKUERS, respectively.  
459 Vehicle emissions i.e. diesel and gasoline engine emissions were the major primary  
460 organic aerosol sources, which contributed to  $28.8 \pm 14.8\%$  and  $37.6 \pm 19.3\%$  of the



461 OC at CP and PKUERS, respectively. Compared with the results of the previous work,  
462 the gasoline engine emission contributed almost twice of that in 2008 (18.0% vs  
463 10.0%), while the contribution of diesel engine emission decreased by 12.5%  
464 compared with the result in 2008. Besides, the contributions of biomass burning and  
465 coal combustion both decreased. The apportioned biogenic and anthropogenic SOC  
466 can explain  $20.2 \pm 6.7\%$  and  $30.5 \pm 12.0\%$  of the measured OC at CP and PKUERS,  
467 respectively. The contribution of toluene SOC is the highest among the apportioned  
468 SOC, which is different from the results of the most developed countries in the world.  
469 Our results revealed an important point, which is that controlling SOA seems feasible  
470 in the developing countries like China. It is difficult to control SOA in developed  
471 countries, since biogenic SOA are dominant. However, deducting anthropogenic  
472 precursors may be an efficient way to reduce the SOA pollution where anthropogenic  
473 SOA is dominant. Back trajectory clustering analysis showed that the particle source  
474 contributions were similar when air masses were from different directions, suggesting  
475 the regional organic particle pollution in Beijing. However, the higher organic particle  
476 loading from south cluster indicates that there were more emissions from southern  
477 region of Beijing. The present work also implied that the aqueous phase  
478 acid-catalyzed reactions may be an important SOA formation mechanism in summer  
479 of Beijing.



480 **Acknowledgement**

481           This research is supported by the National Key R&D Program of China: Task  
482 3 (2016YFC0202000), the National Natural Science Foundation of China (21677002),  
483 framework research program on ‘Photochemical smog in China’ financed by Swedish  
484 Research Council (639-2013-6917).

485 **References**

- 486 Barmpadimos, I., Keller, J., Oderbolz, D., Hueglin, C., and Prévôt, A.: One decade of  
487 parallel fine (PM<sub>2.5</sub>) and coarse (PM<sub>10</sub>–PM<sub>2.5</sub>) particulate matter measurements in  
488 Europe: trends and variability, *Atmos Chem Phys*, 12, 3189–3203, 2012.
- 489 Cao, J. J., Lee, S. C., Ho, K. F., Zou, S. C., Fung, K., Li, Y., Watson, J. G., and Chow,  
490 J. C.: Spatial and seasonal variations of atmospheric organic carbon and  
491 elemental carbon in Pearl River Delta Region, China, *Atmospheric Environment*,  
492 38, 4447–4456, <http://doi.org/10.1016/j.atmosenv.2004.05.016>, 2004.
- 493 Cass, G. R.: Organic molecular tracers for particulate air pollution sources,  
494 *Trac-Trends in Analytical Chemistry*, 17, 356–366,  
495 [10.1016/s0165-9936\(98\)00040-5](http://doi.org/10.1016/s0165-9936(98)00040-5), 1998.
- 496 Cheng, Y., Engling, G., He, K. B., and Duan, F. K.: Biomass burning contribution to  
497 Beijing aerosol, *Atmospheric Chemistry & Physics*, 13, 7765–7781, 2013.
- 498 Cheng, Y., Zheng, G., Wei, C., Mu, Q., Zheng, B., Wang, Z., Gao, M., Zhang, Q., He,  
499 K., and Carmichael, G.: Reactive nitrogen chemistry in aerosol water as a source  
500 of sulfate during haze events in China, *Science Advances*, 2, e1601530, 2016.
- 501 Claeys, M., Graham, B., Vas, G., Wang, W., Vermeylen, R., Pashynska, V., Cafmeyer,  
502 J., Guyon, P., Andreae, M. O., and Artaxo, P.: Formation of Secondary Organic  
503 Aerosols Through Photooxidation of Isoprene, *Science*, 303, 1173, 2004.
- 504 Dan, M., Zhuang, G., Li, X., Tao, H., and Zhuang, Y.: The characteristics of  
505 carbonaceous species and their sources in PM<sub>2.5</sub> in Beijing, *Atmospheric  
506 Environment*, 38, 3443–3452, <http://doi.org/10.1016/j.atmosenv.2004.02.052>,  
507 2004.
- 508 Ding, X., He, Q. F., Shen, R. Q., Yu, Q. Q., and Wang, X. M.: Spatial distributions of  
509 secondary organic aerosols from isoprene, monoterpenes, beta-caryophyllene,  
510 and aromatics over China during summer, *Journal of Geophysical  
511 Research-Atmospheres*, 119, 11877–11891, [10.1002/2014jd021748](http://doi.org/10.1002/2014jd021748), 2014.



- 512 El Haddad, I., Marchand, N., Temime-Roussel, B., Wortham, H., Piot, C., Besombes,  
513 J. L., Baduel, C., Voisin, D., Armengaud, A., and Jaffrezo, J. L.: Insights into the  
514 secondary fraction of the organic aerosol in a Mediterranean urban area:  
515 Marseille, Atmos Chem Phys, 11, 2059-2079, 2011.
- 516 Fu, P., Aggarwal, S. G., Chen, J., Li, J., Sun, Y., Wang, Z., Chen, H., Liao, H., Ding,  
517 A., Umarji, G. S., Patil, R. S., Chen, Q., and Kawamura, K.: Molecular Markers  
518 of Secondary Organic Aerosol in Mumbai, India, Environ. Sci. Technol., 50,  
519 4659-4667, 10.1021/acs.est.6b00372, 2016.
- 520 Gao, J. J., Tian, H. Z., Cheng, K., Lu, L., Wang, Y. X., Wu, Y., Zhu, C. Y., Liu, K. Y.,  
521 Zhou, J. R., Liu, X. G., Chen, J., and Hao, J. M.: Seasonal and spatial variation  
522 of trace elements in multi-size airborne particulate matters of Beijing, China:  
523 Mass concentration, enrichment characteristics, source apportionment, chemical  
524 speciation and bioavailability, Atmospheric Environment, 99, 257-265,  
525 10.1016/j.atmosenv.2014.08.081, 2014.
- 526 Guo, S., Hu, M., Wang, Z. B., Slanina, J., and Zhao, Y. L.: Size-resolved aerosol  
527 water-soluble ionic compositions in the summer of Beijing: implication of  
528 regional secondary formation, Atmos Chem Phys, 10, 947-959, 2010.
- 529 Guo, S., Hu, M., Guo, Q., Zhang, X., Zheng, M., Zheng, J., Chang, C. C., Schauer, J.  
530 J., and Zhang, R.: Primary Sources and Secondary Formation of Organic  
531 Aerosols in Beijing, China, Environmental Science & Technology, 46,  
532 9846-9853, 10.1021/es20425641, 2012.
- 533 Guo, S., Hu, M., Guo, Q., Zhang, X., Schauer, J., and Zhang, R.: Quantitative  
534 evaluation of emission controls on primary and secondary organic aerosol  
535 sources during Beijing 2008 Olympics, Atmos Chem Phys, 13, 8303-8314, 2013.
- 536 Guo, S., Hu, M., Zamora, M. L., Peng, J., Shang, D., Zheng, J., Du, Z., Wu, Z., Shao,  
537 M., and Zeng, L.: Elucidating severe urban haze formation in China, Proceedings  
538 of the National Academy of Sciences, 111, 17373-17378, 2014.



- 539 Haque, M. M., Kawamura, K., and Kim, Y.: Seasonal variations of biogenic  
540 secondary organic aerosol tracers in ambient aerosols from Alaska, *Atmospheric*  
541 *Environment*, 130, 95-104, 10.1016/j.atmosenv.2015.09.075, 2016.
- 542 Hu, D., Bian, Q., Li, T. W., Lau, A. K., and Yu, J. Z.: Contributions of isoprene,  
543 monoterpenes,  $\beta$ -caryophyllene, and toluene to secondary organic aerosols in  
544 Hong Kong during the summer of 2006, *Journal of Geophysical Research:*  
545 *Atmospheres*, 113, 2008.
- 546 Hu, M., Guo, S., Peng, J.-f., and Wu, Z.-j.: Insight into characteristics and sources of  
547 PM<sub>2.5</sub> in the Beijing–Tianjin–Hebei region, China, *National Science Review*, 2,  
548 257-258, 2015.
- 549 Huang, X.-F., He, L.-Y., Hu, M., and Zhang, Y.-H.: Annual variation of particulate  
550 organic compounds in PM<sub>2.5</sub> in the urban atmosphere of Beijing, *Atmospheric*  
551 *Environment*, 40, 2449-2458, 2006.
- 552 Huang, X. F., He, L. Y., Hu, M., Canagaratna, M. R., Sun, Y., Zhang, Q., Zhu, T., Xue,  
553 L., Zeng, L. W., and Liu, X. G.: Highly time-resolved chemical characterization  
554 of atmospheric submicron particles during 2008 Beijing Olympic Games using  
555 an Aerodyne High-Resolution Aerosol Mass Spectrometer, *Atmospheric*  
556 *Chemistry & Physics Discussions*, 10, 8933-8945, 2010.
- 557 Jang, M. S., Czoschke, N. M., Lee, S., and Kamens, R. M.: Heterogeneous  
558 atmospheric aerosol production by acid-catalyzed particle-phase reactions,  
559 *Science*, 298, 814-817, 10.1126/science.1075798, 2002.
- 560 Kleindienst, T. E., Jaoui, M., Lewandowski, M., Offenberg, J. H., Lewis, C. W.,  
561 Bhave, P. V., and Edney, E. O.: Estimates of the contributions of biogenic and  
562 anthropogenic hydrocarbons to secondary organic aerosol at a southeastern US  
563 location, *Atmospheric Environment*, 41, 8288-8300, 2007.
- 564 Kourtchev, I., Warnke, J., Maenhaut, W., Hoffmann, T., and Claeys, M.: Polar organic  
565 marker compounds in PM<sub>2.5</sub> aerosol from a mixed forest site in western  
566 Germany, *Chemosphere*, 73, 1308-1314, 2008.



- 567 Kristensen, K., Cui, T., Zhang, H., Gold, A., Glasius, M., and Surratt, J.: Dimers in  
568  $\alpha$ -pinene secondary organic aerosol: effect of hydroxyl radical, ozone, relative  
569 humidity and aerosol acidity, *Atmos Chem Phys*, 14, 4201-4218, 2014.
- 570 Lambe, A. T., Miracolo, M. A., Hennigan, C. J., Robinson, A. L., and Donahue, N. M.:  
571 Effective Rate Constants and Uptake Coefficients for the Reactions of Organic  
572 Molecular Markers (n-Alkanes, Hopanes, and Steranes) in Motor Oil and Diesel  
573 Primary Organic Aerosols with Hydroxyl Radicals, *Environ. Sci. Technol.*, 43,  
574 8794-8800, 10.1021/es901745h, 2009.
- 575 Liu, Q. Y., Baumgartner, J., Zhang, Y., and Schauer, J. J.: Source apportionment of  
576 Beijing air pollution during a severe winter haze event and associated  
577 pro-inflammatory responses in lung epithelial cells, *Atmospheric Environment*,  
578 126, 28-35, 10.1016/j.atmosenv.2015.11.031, 2016.
- 579 Lough, G. C., Christensen, C. G., Schauer, J. J., Tortorelli, J., Mani, E., Lawson, D. R.,  
580 Clark, N. N., and Gabele, P. A.: Development of molecular marker source  
581 profiles for emissions from on-road gasoline and diesel vehicle fleets, *J. Air  
582 Waste Manage. Assoc.*, 57, 1190-1199, 10.3155/1047-3289.57.10.1190, 2007.
- 583 Miyazaki, Y., Jung, J., Fu, P., Mizoguchi, Y., Yamanoi, K., and Kawamura, K.:  
584 Evidence of formation of submicrometer water - soluble organic aerosols at a  
585 deciduous forest site in northern Japan in summer, *Journal of Geophysical  
586 Research: Atmospheres*, 117, 2012.
- 587 Offenberg, J. H., Lewandowski, M., Edney, E. O., Kleindienst, T. E., and Jaoui, M.:  
588 Influence of Aerosol Acidity on the Formation of Secondary Organic Aerosol  
589 from Biogenic Precursor Hydrocarbons, *Environ. Sci. Technol.*, 43, 7742-7747,  
590 10.1021/es901538e, 2009.
- 591 Oros, D. R., and Simoneit, B. R. T.: Identification and emission rates of molecular  
592 tracers in coal smoke particulate matter, *Fuel*, 79, 515-536, Doi  
593 10.1016/S0016-2361(99)00153-2, 2000.



- 594 Park, S. S., and Cho, S. Y.: Tracking sources and behaviors of water-soluble organic  
595 carbon in fine particulate matter measured at an urban site in Korea, *Atmospheric*  
596 *environment*, 45, 60-72, 2011.
- 597 Rogge, W. F., Hildemann, L. M., Mazurek, M. A., Cass, G. R., and Simoneit, B. R. T.:  
598 Sources of fine organic aerosol. 4. Particulate abrasion products from leaf  
599 surfaces of urban plants, *Environ. Sci. Technol.*, 27, 2700-2711, 1993.
- 600 Saathoff, H., Naumann, K.-H., Möhler, O., Jonsson, Å. M., Hallquist, M.,  
601 Kiendler-Scharr, A., Mentel, T. F., Tillmann, R., and Schurath, U.: Temperature  
602 dependence of yields of secondary organic aerosols from the ozonolysis of  
603  $\alpha$ -pinene and limonene, *Atmos Chem Phys*, 9, 1551-1577, 2009.
- 604 Schauer, J. J., Rogge, W. F., Hildemann, L. M., Mazurek, M. A., Cass, G. R., and  
605 Simoneit, B. R. T.: Source apportionment of airborne particulate matter using  
606 organic compounds as tracers, *Atmospheric Environment*, 30, 3837-3855,  
607 10.1016/1352-2310(96)00085-4, 1996.
- 608 Sheesley, R. J., Schauer, J. J., Zheng, M., and Wang, B.: Sensitivity of molecular  
609 marker-based CMB models to biomass burning source profiles, *Atmospheric*  
610 *Environment*, 41, 9050-9063, 2007.
- 611 Simoneit, B. R., Schauer, J. J., Nolte, C., Oros, D. R., Elias, V. O., Fraser, M., Rogge,  
612 W., and Cass, G. R.: Levoglucosan, a tracer for cellulose in biomass burning and  
613 atmospheric particles, *Atmospheric Environment*, 33, 173-182, 1999.
- 614 Song, G., Min, H., Qingfeng, G., and Dongjie, S.: Comparison of secondary organic  
615 aerosol estimation methods, *ACTA CHIMICA SINICA*, 72, 658-666, 2014.
- 616 Song, Y., Zhang, Y., Xie, S., Zeng, L., Zheng, M., Salmon, L. G., Shao, M., and  
617 Slanina, S.: Source apportionment of PM<sub>2.5</sub> in Beijing by positive matrix  
618 factorization, *Atmospheric Environment*, 40, 1526-1537, 2006.
- 619 Stone, E. A., Nguyen, T. T., Pradhan, B. B., and Dangol, P. M.: Assessment of  
620 biogenic secondary organic aerosol in the Himalayas, *Environmental Chemistry*,  
621 9, 263-272, 2012.



- 622 Sun, J., Zhang, Q., Canagaratna, M. R., Zhang, Y., Ng, N. L., Sun, Y., Jayne, J. T.,  
623 Zhang, X., Zhang, X., and Worsnop, D. R.: Highly time- and size-resolved  
624 characterization of submicron aerosol particles in Beijing using an Aerodyne  
625 Aerosol Mass Spectrometer, *Atmospheric Environment*, 44, 131-140, 2010.
- 626 Surratt, J. D., Kroll, J. H., Kleindienst, T. E., Edney, E. O., Claeys, M., Sorooshian, A.,  
627 Ng, N. L., Offenberg, J. H., Lewandowski, M., Jaoui, M., Flagan, R. C., and  
628 Seinfeld, J. H.: Evidence for organosulfates in secondary organic aerosol,  
629 *Environ. Sci. Technol.*, 41, 517-527, 10.1021/es062081q, 2007.
- 630 Surratt, J. D., Chan, A. W., Eddingsaas, N. C., Chan, M., Loza, C. L., Kwan, A. J.,  
631 Hersey, S. P., Flagan, R. C., Wennberg, P. O., and Seinfeld, J. H.: Reactive  
632 intermediates revealed in secondary organic aerosol formation from isoprene,  
633 *Proceedings of the National Academy of Sciences*, 107, 6640-6645, 2010.
- 634 Tai, A. P., Mickley, L. J., and Jacob, D. J.: Correlations between fine particulate matter  
635 (PM 2.5) and meteorological variables in the United States: Implications for the  
636 sensitivity of PM 2.5 to climate change, *Atmospheric Environment*, 44,  
637 3976-3984, 2010.
- 638 Tan, J. H., Duan, J. C., Chai, F. H., He, K. B., and Hao, J. M.: Source apportionment  
639 of size segregated fine/ultrafine particle by PMF in Beijing, *Atmospheric  
640 Research*, 139, 90-100, 10.1016/j.atmosres.2014.01.007, 2014.
- 641 Tao, J., Zhang, L., Cao, J., Zhong, L., Chen, D., Yang, Y., Chen, D., Chen, L., Zhang,  
642 Z., Wu, Y., Xia, Y., Ye, S., and Zhang, R.: Source apportionment of PM<sub>2.5</sub> at  
643 urban and suburban areas of the Pearl River Delta region, south China - With  
644 emphasis on ship emissions, *Science of the Total Environment*, 574, 1559-1570,  
645 10.1016/j.scitotenv.2016.08.175, 2017.
- 646 Tian, S. L., Pan, Y. P., and Wang, Y. S.: Size-resolved source apportionment of  
647 particulate matter in urban Beijing during haze and non-haze episodes, *Atmos  
648 Chem Phys*, 16, 1-19, 10.5194/acp-16-1-2016, 2016.



- 649 Wang, Q., Shao, M., Zhang, Y., Wei, Y., Hu, M., and Guo, S.: Source apportionment  
650 of fine organic aerosols in Beijing, *Atmospheric Chemistry and Physics*, 9,  
651 8573-8585, 2009.
- 652 Wang, X., Bi, X., Sheng, G., and Fu, J.: Chemical composition and sources of PM10  
653 and PM2.5 aerosols in Guangzhou, China, *Environmental Monitoring and*  
654 *Assessment*, 119, 425-439, 2006.
- 655 Wong, J. P. S., Lee, A. K. Y., and Abbatt, J. P. D.: Impacts of Sulfate Seed Acidity and  
656 Water Content on Isoprene Secondary Organic Aerosol Formation, *Environ. Sci.*  
657 *Technol.*, 49, 13215-13221, [10.1021/acs.est.5b02686](https://doi.org/10.1021/acs.est.5b02686), 2015.
- 658 Wu, Y., Guo, J., Zhang, X., and Li, X.: Correlation between PM concentrations and  
659 Aerosol Optical Depth in eastern China based on BP neural networks,  
660 *Geoscience and Remote Sensing Symposium*, 2011, 5876-5886.
- 661 Xiang, P., Zhou, X. M., Duan, J. C., Tan, J. H., He, K. B., Yuan, C., Ma, Y. L., and  
662 Zhang, Y. X.: Chemical characteristics of water-soluble organic compounds  
663 (WSOC) in PM2.5 in Beijing, China: 2011-2012, *Atmos. Res.*, 183, 104-112,  
664 [10.1016/j.atmosres.2016.08.020](https://doi.org/10.1016/j.atmosres.2016.08.020), 2017.
- 665 Yang, F., Kawamura, K., Chen, J., Ho, K. F., Lee, S. C., Gao, Y., Cui, L., Wang, T. G.,  
666 and Fu, P. Q.: Anthropogenic and biogenic organic compounds in summertime  
667 fine aerosols (PM2.5) in Beijing, China, *Atmospheric Environment*, 124,  
668 166-175, [10.1016/j.atmosenv.2015.08.095](https://doi.org/10.1016/j.atmosenv.2015.08.095), 2016.
- 669 Yttri, K. E., Simpson, D., Nojgaard, J. K., Kristensen, K., Genberg, J., Stenstrom, K.,  
670 Swietlicki, E., Hillamo, R., Aurela, M., Bauer, H., Offenberg, J. H., Jaoui, M.,  
671 Dye, C., Eckhardt, S., Burkhardt, J. F., Stohl, A., and Glasius, M.: Source  
672 apportionment of the summer time carbonaceous aerosol at Nordic rural  
673 background sites, *Atmos Chem Phys*, 11, 13339-13357, 2011.
- 674 Yu, L. D., Wang, G. F., Zhang, R. J., Zhang, L. M., Song, Y., Wu, B. B., Li, X. F., An,  
675 K., and Chu, J. H.: Characterization and Source Apportionment of PM2.5 in an



- 676 Urban Environment in Beijing, *Aerosol Air Qual Res*, 13, 574-583,  
677 10.4209/aaqr.2012.07.0192, 2013.
- 678 Zhang, H., Zhang, Z., Cui, T., Lin, Y.-H., Bhathela, N. A., Ortega, J., Worton, D. R.,  
679 Goldstein, A. H., Guenther, A., Jimenez, J. L., Gold, A., and Surratt, J. D.:  
680 Secondary Organic Aerosol Formation via 2-Methyl-3-buten-2-ol Photooxidation:  
681 Evidence of Acid-Catalyzed Reactive Uptake of Epoxides, *Environmental*  
682 *Science & Technology Letters*, 1, 242-247, 10.1021/ez500055f, 2014.
- 683 Zhang, Q., Streets, D. G., Carmichael, G. R., He, K. B., Huo, H., Kannari, A.,  
684 Klimont, Z., Park, I. S., Reddy, S., Fu, J. S., Chen, D., Duan, L., Lei, Y., Wang, L.  
685 T., and Yao, Z. L.: Asian emissions in 2006 for the NASA INTEX-B mission,  
686 *Atmos Chem Phys*, 9, 5131-5153, 2009.
- 687 Zhang, R., Jing, J., Tao, J., Hsu, S.-C., Wang, G., Cao, J., Lee, C. S. L., Zhu, L., Chen,  
688 Z., and Zhao, Y.: Chemical characterization and source apportionment of PM 2.5  
689 in Beijing: seasonal perspective, *Atmos Chem Phys*, 13, 7053-7074, 2013.
- 690 Zhang, Y., Cai, J., Wang, S., He, K., and Zheng, M.: Review of receptor-based source  
691 apportionment research of fine particulate matter and its challenges in China,  
692 *The Science of the total environment*, 586, 917-929,  
693 10.1016/j.scitotenv.2017.02.071, 2017.
- 694 Zheng, J., Hu, M., Peng, J., Wu, Z., Kumar, P., Li, M., Wang, Y., and Guo, S.: Spatial  
695 distributions and chemical properties of PM 2.5 based on 21 field campaigns at  
696 17 sites in China, *Chemosphere*, 159, 480-487, 2016a.
- 697 Zheng, M., Salmon, L. G., Schauer, J. J., Zeng, L., Kiang, C., Zhang, Y., and Cass, G.  
698 R.: Seasonal trends in PM<sub>2.5</sub> source contributions in Beijing, China,  
699 *Atmospheric Environment*, 39, 3967-3976, 2005.
- 700 Zheng, X. X., Guo, X. Y., Zhao, W. J., Shu, T. T., Xin, Y. A., Yan, X., Xiong, Q. L.,  
701 Chen, F. T., and Lv, M.: Spatial variation and provenance of atmospheric trace  
702 elemental deposition in Beijing, *Atmos. Pollut. Res.*, 7, 260-267,  
703 10.1016/j.apr.2015.10.006, 2016b.



- 704 Zhou, J. B., Xiong, Y., Xing, Z. Y., Deng, J. J., and Du, K.: Characterizing and  
705 sourcing ambient PM<sub>2.5</sub> over key emission regions in China II: Organic  
706 molecular markers and CMB modeling, *Atmospheric Environment*, 163, 57-64,  
707 10.1016/j.atmosenv.2017.05.033, 2017.
- 708 Zhu, C., Kawamura, K., and Fu, P.: Seasonal variations of biogenic secondary organic  
709 aerosol tracers in Cape Hedo, Okinawa, *Atmospheric Environment*, 130, 113-119,  
710 10.1016/j.atmosenv.2015.08.069, 2016.
- 711 Zhu, Y., Yang, L., Kawamura, K., Chen, J., Ono, K., Wang, X., Xue, L., and Wang, W.:  
712 Contributions and source identification of biogenic and anthropogenic  
713 hydrocarbons to secondary organic aerosols at Mt. Tai in 2014, *Environmental*  
714 *Pollution*, 220, 863-872, 10.1016/j.envpol.2016.10.070, 2017.



### Table

Table 1. Summer PM<sub>2.5</sub> mass concentrations in Beijing from 2008-2016, average ± standard deviation (μg m<sup>-3</sup>).

Year/Mont h	2008/07	2009/07	2010/05	2016/05-06	2016/05-06
Site	PKUERS	PKUERS	PKUERS	CP	PKUERS
	(μg m <sup>-3</sup> )	(μg m <sup>-3</sup> )	(μg m <sup>-3</sup> )	(μg m <sup>-3</sup> )	(μg m <sup>-3</sup> )
PM <sub>2.5</sub>	92.3±44.7	88.2±52.3	62.7±36.5	43.0±17.5	45.5±19.8
OC	10.4±2.9	8.5±2.5	8.9±4.5	8.9±3.2	11.0±3.7
EC	3.3±1.5	2.5±0.9	2.1±1.1	0.7±0.5	1.8±1.0
Ref.	(Guo et al., 2012)	(Zheng et al., 2016a)	(Zheng et al., 2016a)	This study	This study



### Figure captions

Fig. 1 Concentrations of organic carbon from primary and secondary organic sources at (a) CP and (b) PKUERS as well as their contributions to the measured organic carbon at (c) CP and (d) PKUERS (%).

Fig. 2 Comparison of the sources at PKUERS between 2016 and 2008

Fig. 3 Particle sources from different air mass origins

Fig. 4 Correlations between SOC and different influencing factors (a)-(b) ozone, (c)-(d) temperature, (e)-(f) water and (g)-(h)  $H^+$  concentratio

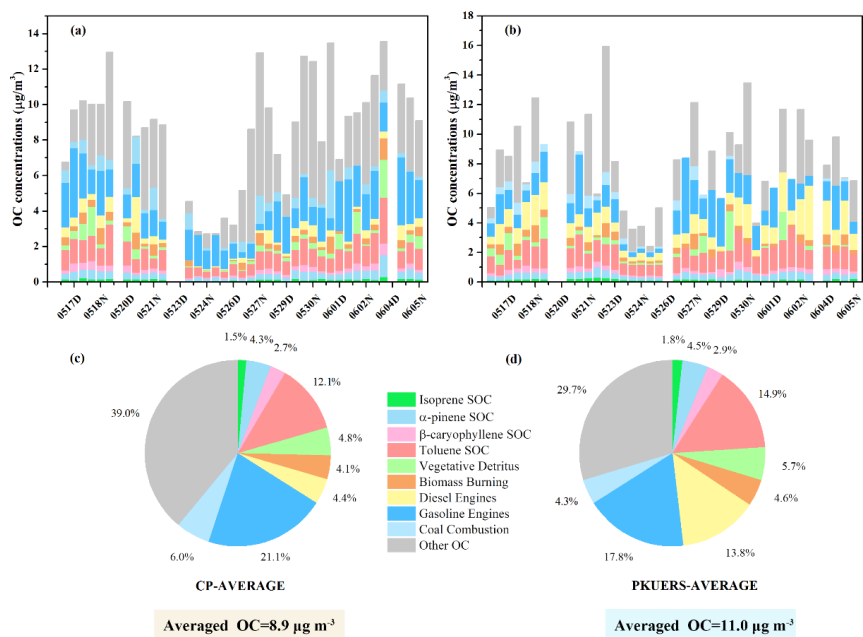


Fig. 1 Concentrations of organic carbon from primary and secondary organic sources at (a) CP and (b) PKUERS as well as their contributions to the measured organic carbon at (c) CP and (d) PKUERS (%).

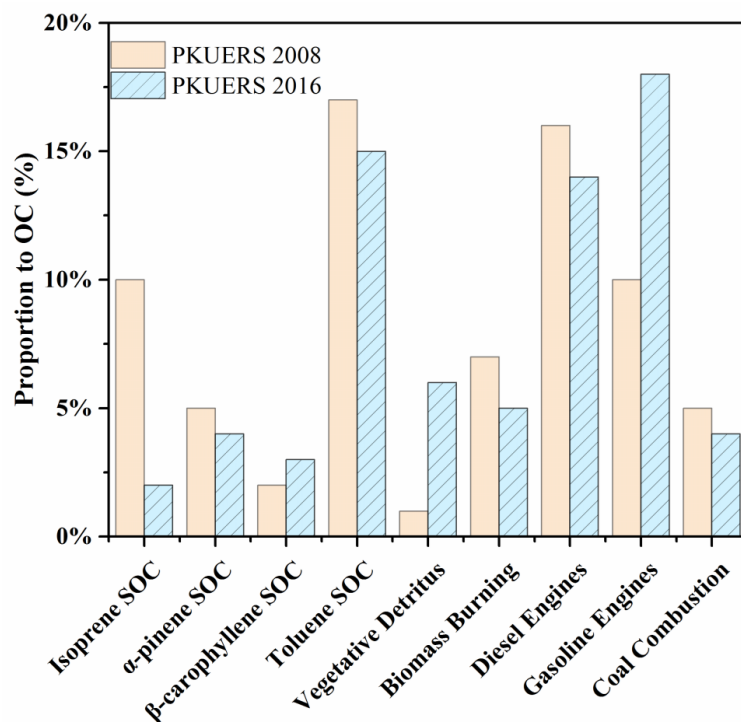


Fig.2 Comparison of the sources at PKUERS between 2016 and 2008 (Guo et al. 2012)

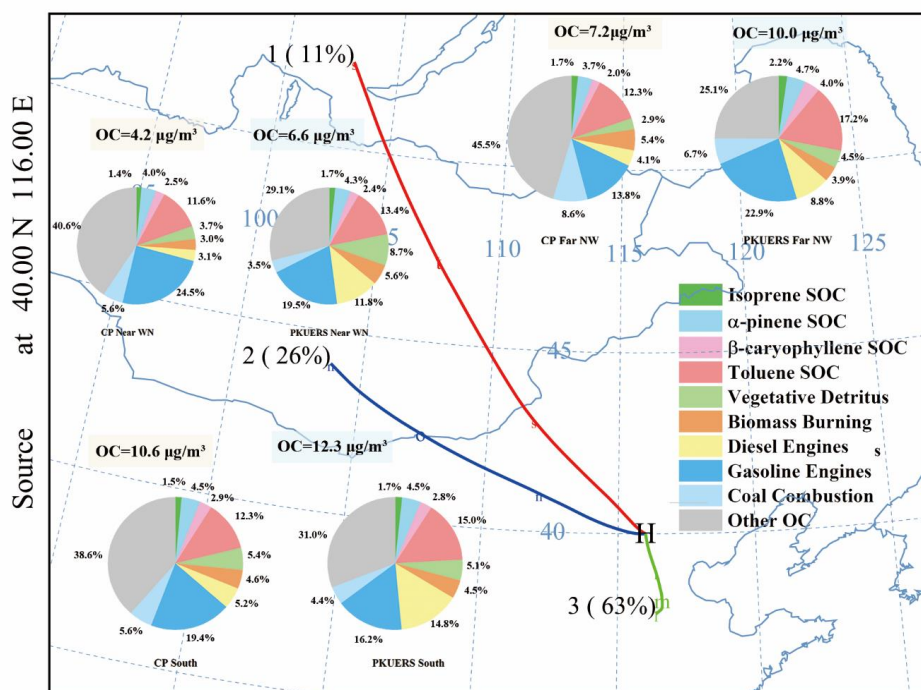


Fig. 3 Particle sources from different air mass origins

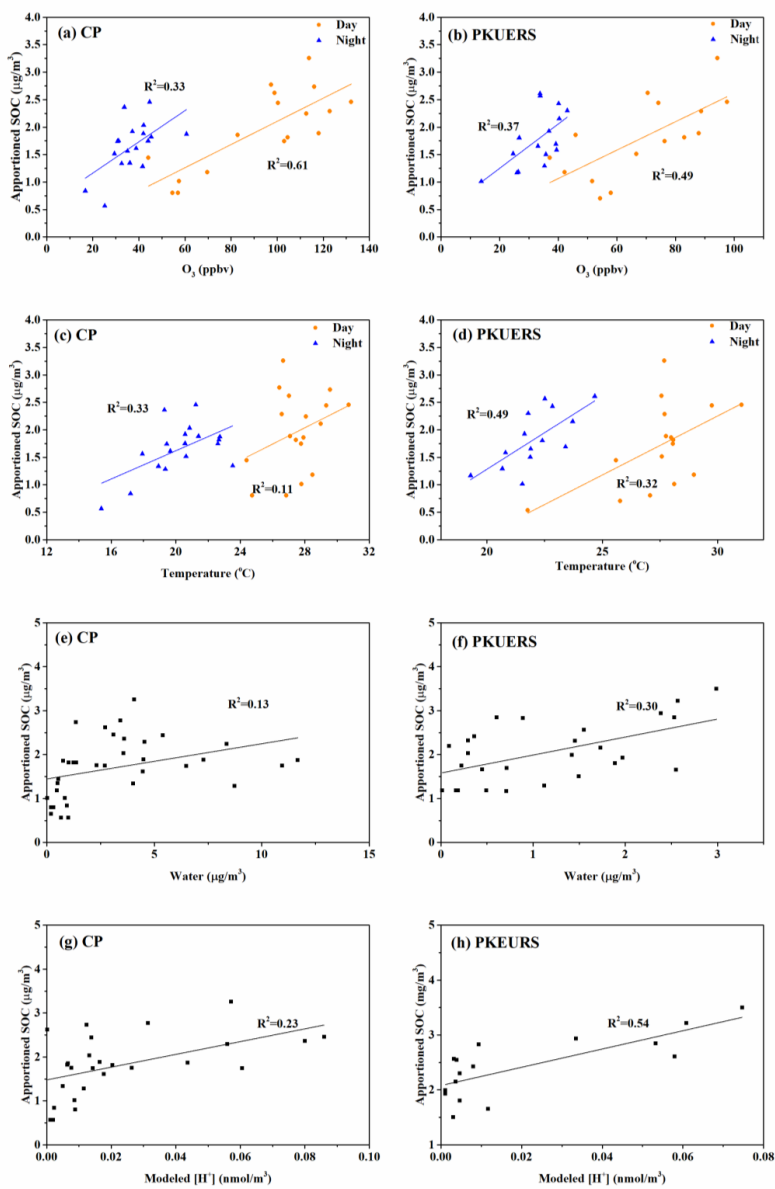


Fig. 4 Correlations between SOC and different influencing factors (a)-(b) ozone, (c)-(d) temperature, (e)-(f) water and (g)-(h)  $H^+$  concentration